Article

Versatile Cell and Animal Models for Advanced Investigation of Lead Poisoning

De-Ming Yang [1,2,*] **and Yu-Fen Chang** [3]

[1] Microscopy Service Laboratory, Basic Research Division, Department of Medical Research, Taipei Veterans General Hospital, Taipei, Taiwan; dmyang@vghtpe.gov.tw
[2] Institute of Biophotonics, School of Biomedical Science and Engineering National Yang Ming Chiao Tung University, Taipei, Taiwan; yang.deming2021@nycu.edu.tw
[3] LumiSTAR Biotechnology, Inc., Taipei City 115, Taiwan; yu-fen.chang@lumistar.com.tw
* Correspondence: dmyang@vghtpe.gov.tw

Abstract: The heavy metal lead (Pb) can irreversibly damage the human nervous system. To help understand Pb-induced damage, we have developed practical applications for genetically encoded Pb biosensors in cardiac cells and insect central nervous tissue. We applied the optimized fluorescence resonance energy transfer (FRET)-based Pb biosensor Met-lead 1.44 M1 to two living systems to monitor the concentration of Pb: induced pluripotent stem cell (iPSC)-derived cardiomyocytes as a semi-tissue platform, and *Drosophila melanogaster* fruit flies as an *in vivo* animal model. Different FRET imaging modalities were used to obtain FRET signals, which represented the presence of Pb in the tested samples in different spatial dimensions. Pb was effectively sensed in two living models producing Met-led 1.44 M1. In iPSC-derived cardiomyocytes, the relationship between beating rate determined from the fluctuation of fluorescent signals and the concentrations of Pb represented by the FRET emission ratio values of Met-lead 1.44 M1 demonstrated the potential of this fluorescence biosensor system for anti-Pb drug screening. In the *Drosophila* model, Pb was detected within the adult brain or larval central nervous system using fast epifluorescence and high-resolution two-photon 3D FRET ratio image systems. The optimized Pb biosensor together with FRET microscopy can be used for specific applications to detect Pb with a limit of detection of 10 nM (2 ppb). We believe that this integrated Pb biosensor system can be applied to the prevention of Pb poisoning.

Keywords: *Drosophila melanogaster*, fluorescence resonance energy transfer, Met-lead 1.44 M1, Pb biosensor

1. Introduction

Toxic elements such as the heavy metal lead (Pb) have been affecting the daily lives of humans for more than three thousand years. Pb has been used to adulterate wine and gasoline, to make water pipes (since the ancient Roman period), in traditional Chinese medicine, and as a component of glass and ceramics, paint, hair dyes, children's toys, and batteries. The recognition that Pb damages human tissues was only reached after countless sad historical events. For example, during the last Arctic expedition of Sir John Franklin in 1845, all the crew members of the ships *Erebus* and *Terror* were found dead two years after they had gone missing. Detailed investigations suggested that in addition to tuberculosis, Pb poisoning from contaminated tinned food and water was an important factor in these deaths [1-6]. The neurological effects of high Pb exposure include delusion, impaired judgment, and even a desire to commit murder. An increased Pb content in honey produced near the Cathedral of Notre-Dame de Paris in France after a 2019 fire was found to derive from old leaded stained glass that was destroyed by the fire, producing fumes that were spread by the wind [7-9]. More recently, a doctor of Chinese medicine in Taiwan illegally issued an incorrect prescription containing large amounts of Pb, which led to harmful effects for patients with ages ranging from 4 to 85 years old. Pb can cause tissue damage that leads to neurological disorders, including cognitive deficits, low intelligence

quotient (IQ), and attention-deficit hyperactivity disorder (ADHD) [10]. In addition, Pb can cause cardiovascular diseases (CVDs) such as secondary arterial hypertension [11], and circulatory illnesses including anemia [12]. These toxicological impacts of Pb can result from various pathways of Pb exposure, such as drinking contaminated water, breathing, eating, and physical contact with Pb.

Fluorescent indicators in combination with suitable readout platforms can be used to monitor the presence of specific compounds or elements within living systems or in their environment [13,14]. These indicators can be in chemical form, which are preferentially applied for environmental sensing; alternatively, they can be genetically encoded (GE), as with fluorescent protein (FP) biosensors that can be expressed intracellularly to sense specific targets. Strategies for the qualitative and quantitative sensing of targets by GEFP biosensors can include the combination of a bioreceptor (a selected sensing domain) with a signal transducer, which transforms target recognition events into fluorescent signals. For example, the first GEFP biosensor, cameleon, was developed to detect fluorescence resonance energy transfer (FRET) signal events between two pairs of FPs (BFP with GFP, or CFP with YFP) following the sensing of intracellular calcium ions [15]. This novel strategy makes it possible to visualize specific molecules in real time and in a genetically controlled manner without the need to stain tissues.

This strategy inspired the development of different types of FRET-based biosensors round the world to examine the dynamic status of living cells and thus better understand the functional roles of molecules of interest, to precisely and rapidly predict the fate of targeted cells, and, in particular, to provide a powerful platform for drug screening [16,17]. Because they require high molecular selectivity, however, GEFP biosensors to detect metal ions, such as zinc (Zn^{2+}), copper (Cu^{2+}), silver (Ag^+), cadmium (Cd^{2+}), and Pb^{2+}, have been relatively difficult to generate [18-23]. Given the importance of monitoring heavy metals in environmental and biological samples, biosensors that can perform both these functions are especially desirable.

To monitor Pb toxicity, we designed the FRET-based GEFP biosensor Met-lead (Figure 1), which we reported previously [20]. However, the sensing ability of the first version, Met-lead 1.59 (Figure 1A), provided a dynamic range (DR) of less than two-fold and a limit of detection (LOD) of about 500 nM (~10 μg/dL; compared with a recommended maximum blood lead level for children of 2 μg/dL), making it unsuitable for further applications [20]. Therefore, we endeavored to improve the sensitivity of Met-lead molecules in different ways, including adjusting the lengths of the Pb-sensing domains and inserting a repeat sequence (linker) in the center of the Pb-sensing domains [23]. We achieved a LOD of Pb of 10 nM (2 ppb) for the most recent Met-lead version, 1.44 M1 (Figure 1B). This offers great potential for important practical applications such as the detection of Pb in the environment (in water for drinking or irrigation), in body fluids (in cells, serum, or urine) or in other tissues (*in vivo* in whole animals or plants), filling a need that has been widely noted by researchers over the years. In this study, we used two different systems to demonstrate the measurement of Pb under various conditions: induced pluripotent stem cell (iPSC)-derived cardiomyocytes [24,25] with measurable functional parameters, which provide a unique *in vitro* tissue model, and the adult brain and larval central nervous system (CNS) of transgenic *Drosophila*, as an easy-to-handle *in vivo* model [23,26].
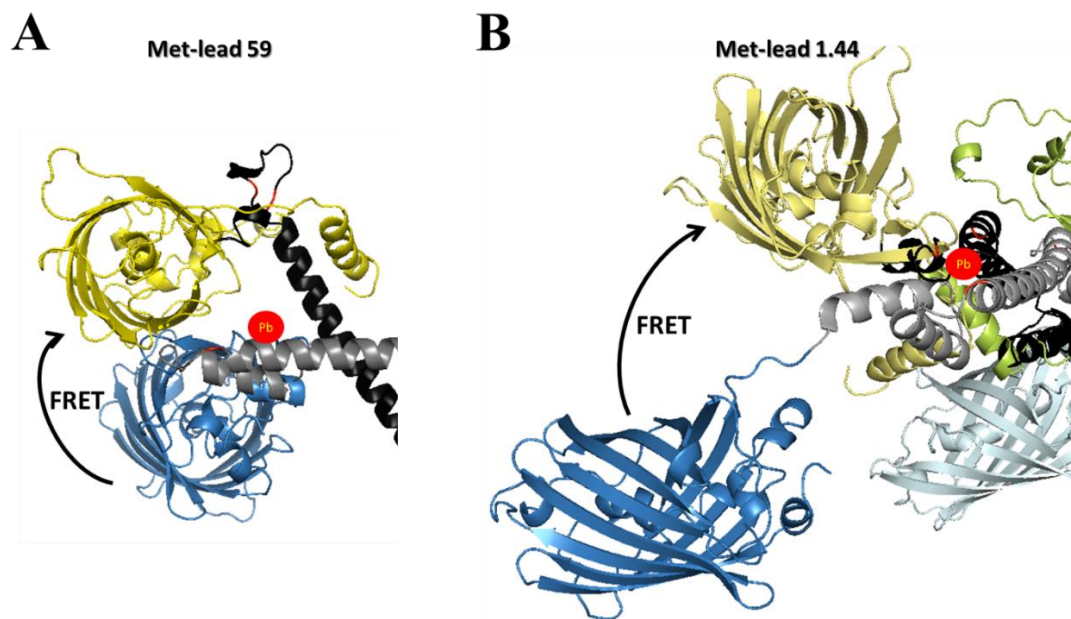
Figure 1. The simulated structure of FRET-based Met-lead Pb sensors. A, B, The FRET pair of fluorescent proteins within Met-lead (A, version 1.59; B, version 1.44) are depicted: ECFP (blue) and EYFP (yellow) led to FRET in the presence of the target (Pb, red circles), due to Pb binding by the sensing key residues (three red lines near Pb). This image was adapted from a previous report [28].

2. Results

2.1. Simultaneous monitoring of physical cardiomyocyte activity and Pb content

The cardiovascular system is one of the most important targets of Pb toxicity [27,28]. The entry of Pb into the cardiovascular system has been suggested to occur via various calcium (Ca^{2+}) channels [29,30], and Pb impairs the normal function of cardiac contraction [27,31,32]. We used the improved Met-lead 1.44 M1 Pb biosensor in iPSC-derived cardiomyocytes to demonstrate the sensing ability of Met-lead (FRET ratio increase; Figure 2F, G) while simultaneously obtaining physiological parameters (e.g. the cardiomyocyte beating rate; Figure 2D, E). The beating frequency of the cardiomyocytes was significantly affected by exposure to Pb (50 µM; Figure 2F, G; Table 1). Pretreatment with the calcium channel blocker verapamil (2 µM) not only impaired the beating function of cardiomyocytes (Figure 3D and Table 1), but also decreased the entry of Pb (Figure 3F and Table 1). Another calcium channel blocker, 2-aminoethoxydiphenyl borate (2-APB; 50 µM; the store-operated Ca-channel inhibitor), altered the rate of beating (Figure 3E and Table 1) without stopping beating as verapamil did (Figure 3D and Table 1). This experiment provided a time-lapse recording of Met-lead as a classical demonstration of *in situ* Pb monitoring, and also generated additional information about the health status (beating rate) of living cardiomyocytes.

Table 1. Intracellular entry of Pb (FRET ratio changes) and the physiological impact of Pb (beating rate) on iPSC-induced cardiomyocytes. The original data were extracted from Figures 2 and 3.

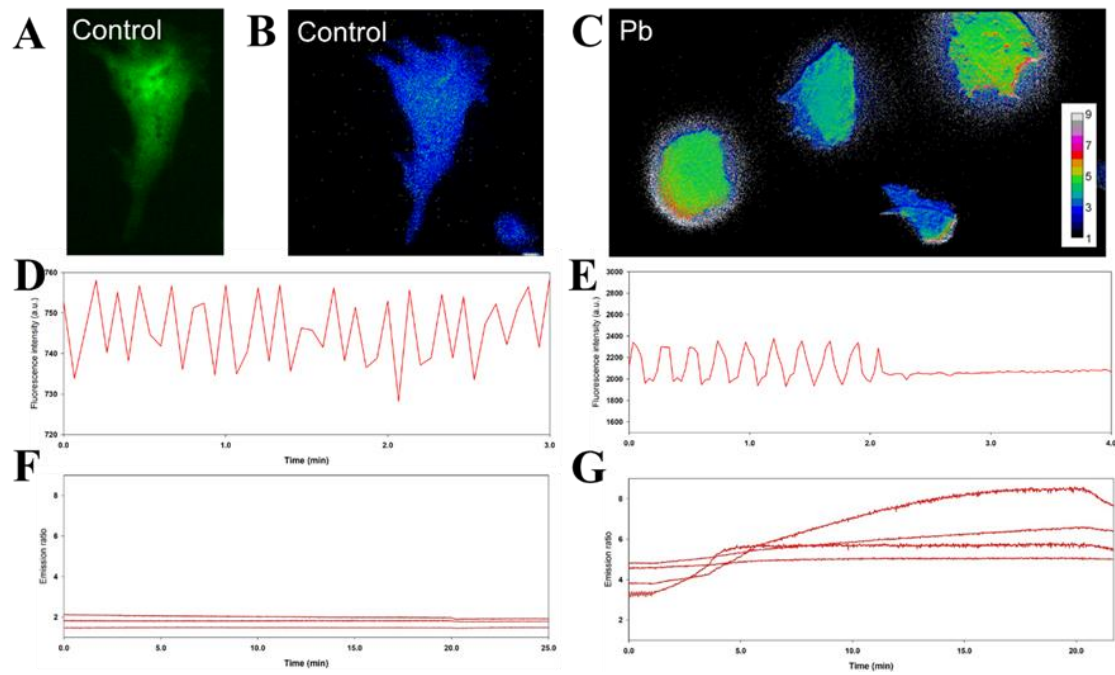| iPSC experimental sets	Delta Pb (FRET ratio)	Beating frequency
Control	NA[1] (basal maintained at 1.97±0.15)	6 Hz → 6 Hz
Pb (50 µM)	2.06 (4.18±0.32 → 6.24±0.17)	5 Hz → NA
Pb (50 µM) + Verapamil	0.19 (3.06±0.14 → 3.25±0.73)	NA
Pb (50 µM) + 2-APB	0.34 (1.91±0.1 → 2.25±0.47)	6 Hz → 6 Hz

[1] NA: none detected.

Figure 2. The simultaneous recording of the physiological activity and entry of Pb into iPSC-derived cardiomyocytes. A–C, The fluorescence and FRET ratio images of cells expressing Met-lead 1.44 M1 were acquired in control buffer (A and B) or after Pb treatment (50 μM; C). The color bar for B and C represents ratio values from 1 to 9. D, E, Within the 25-min recordings, the time-lapse fluctuation of fluorescence signals in the tested cells revealed the beating activity (control in D; Pb in E). F, G, Simultaneously, intracellular Pb sensing could be observed in control (F) and Pb (G) treatments.
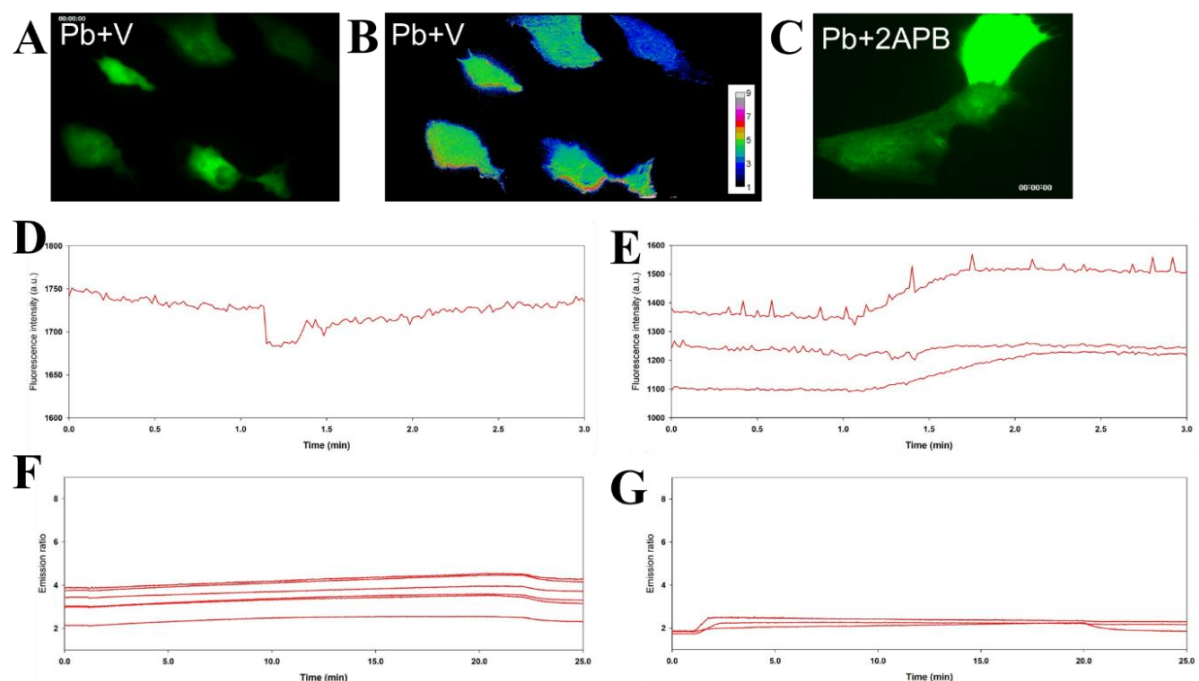

Figure 3. Assessment of the differential effects of Ca²⁺ blockers on iPSC-derived cardiomyocytes by the simultaneous recording of beating activity and Pb sensing. A–C, The fluorescence and FRET ratio images of cells expressing Met-lead 1.44 M1 were acquired in Pb buffer with verapamil (P+V; A and B) or in Pb buffer with 2-aminoethoxydiphenyl borate (2-APB) (P+2APB; C). The color bar in B represents ratio values from 1 to 9. D, E, During the 25-min recordings, the time-lapse fluctuation in fluorescence signals in the tested cells revealed the beating activity (D and E). F, G, Intracellular Pb sensing can be observed for Pb in the presence of verapamil (F) and for Pb in the presence of 2-APB (G).

2.2. In vivo Pb sensing

The impact of Pb on the nervous system has been noted for years [10,12]. In this study, we introduced the improved Met-lead 1.44 M1 (Figure 1B) biosensor gene into *Drosophila* with tissue-specific expression of the upstream activating sequence controlling the gene's expression (UAS-GAL4 flies). In this way, the performance of the Pb biosensor within targeted organs at different life stages, such as the adult brain (Figure 4) or larval CNS (Figure 5), could be detected. In adult flies that expressed the Pb biosensor within cholinergic neurons (*Cha-gal4 > UAS-Met-lead 1.44 M1*, Figure 4A, B), changes in the FRET ratio signal within the neurons of the brain were visualized as rainbow-colored images (Figure 4C) or were displayed as line plots for selected regions (Figure 4D). These increased FRET ratio signals not only represent the presence of Pb *in situ* (Figure 4C, D), but also provide a direct demonstration that the Pb biosensor can be used to detect the Pb content within living organisms.
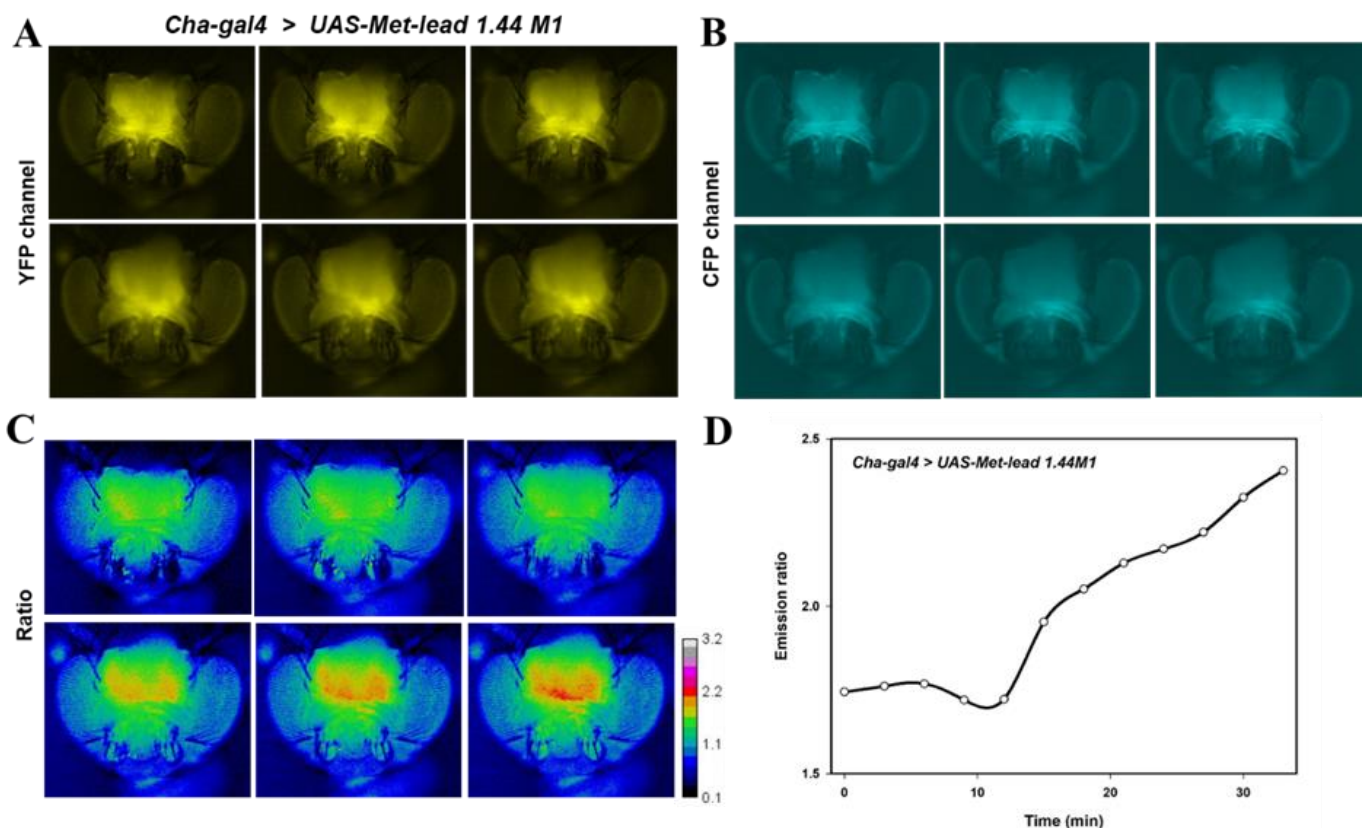

Figure 4. *In vivo* **Pb biosensing in the adult brain of *Drosophila* (strain *Cha-gal4 > UAS-Met-lead 1.44 M1*) using FRET ratio live imaging.** A–C, Representative fluorescence images of YFP (A) and CFP (B) emission, and the emission ratio (YFP/CFP, C), in the fly brain during a 35-min recording. The color bar in C represents ratio values from 0.1 to 3.2. D, Time-lapse changes in the emission ratio value (YFP/CFP) during the *in vivo* recording.

We also used two-photon FRET imaging to monitor the concentration of Pb within the intact larval CNS (*Cha-gal4 > UAS-Met-lead 1.44 M1*, Figure 5) in a 3D manner (Figure 5A) or using sectional imaging (Figure 5B; for representative sections). The ratio values within different regions of interest along vertical sections of the larval CNS are shown in Figure 5C.
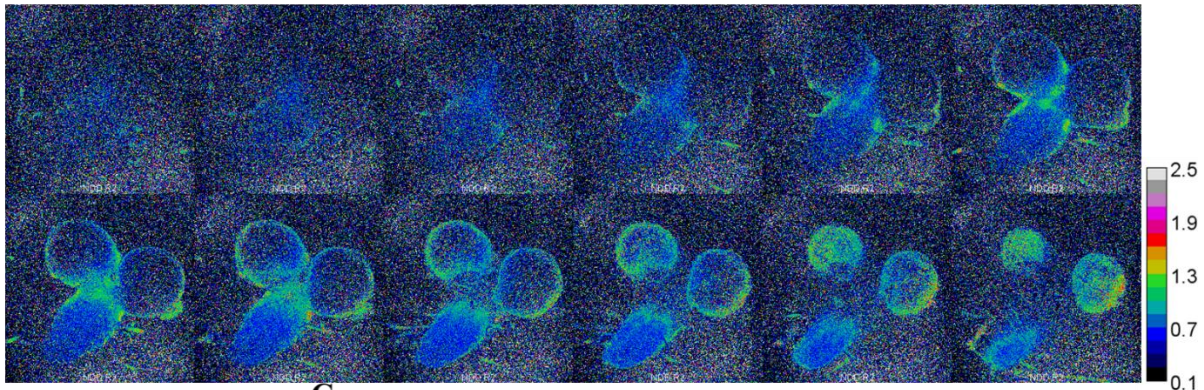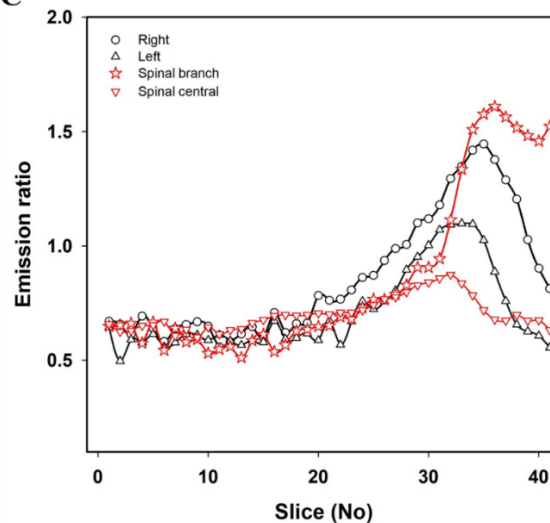
Figure 5. *In vivo* **Pb biosensing in the larval CNS of** *Drosophila* **using high-resolution two-photon FRET ratio imaging.** A, A 3D reconstructed (projection) image of the larval CNS taken using a two-photon DRET ratio microscope (40 sections in total) was rotated by 360°. B, Twelve representative sections are shown. C, The emission ratio values of these 3D-sectioned FRET images are displayed for different depths (slice number) and certain regions were selected, such as the right (○) and left (△) parts of the larval brain hemisphere and the branch (☆) and center (▽) of the spinal cord. The color bar in B represents ratio values from 0.1 to 2.5.

3. Discussion

Although the use and acceptable concentrations of Pb are highly regulated, Pb continues to harm human health and cause neurological disorders [10] and/or CVDs [11], even at relatively low levels that may be under the critical limit allowed in a particular jurisdiction [10,12]. An advanced tool to indicate the presence of Pb in the environment or in human daily inputs such water, food and merchandise would be extremely beneficial.

In this study, we demonstrate practical applications of the optimized FRET-based genetically encoded Pb biosensor Met-lead 1.44 M1 (Figure 1B) in two different systems: *in vitro* in iPSC-derived cardiomyocytes (Figure 2 and 3) and *in vivo* in fruit flies (Figure 4 and 5).

The activity of cardiomyocytes was simultaneously monitored during the detection of Pb. Because concerns exists about the use of chelating agents such as dimercaprol (British anti-Lewisite, BAL) and calcium disodium ethylenediaminetetraacetic acid (CaEDTA) to treat Pb poisoning [33,34], it would be useful to identify alternative drugs that can remove Pb from human tissues such as cardiomyocytes with the fewest side-effects. The combination of Met-lead 1.44 M1 with iPSC-derived cardiomyocytes provides a good platform with which to search for candidate anti-Pb drugs while simultaneously monitoring the cardiac toxicity of Pb by measuring beating activity (Figure 2D, E; Figure 3D, E; Table 1). The development of a Pb-monitoring system that can also sense cardiac activity through its incorporation of a near-infrared genetically encoded calcium ion biosensor (NIR-GECO1) [35] may achieve this aim in the future, because the spectrum of NIR-GECO1 does not overlap with that of Met-lead (CFP and YFP).

Our work here also served to introduce a promising animal model for studying Pb poisoning: Because the *UAS-Gal4* system can be used to express the genetically encoded Pb biosensor in a tissue-specific manner, the *UAS-Met-lead 1.44 M1* fly strain can be used for further toxicological investigations of Pb-sensitive organs. For example, the influence of Pb on neuronal activity or circuitry can be revealed by monitoring neurons that express Met-lead, such as cholinergic neurons in adult (Figure 4) or larval flies (Figure 5). The use of 3D microscopic imaging of single cells, together with FRET Pb biosensing, can create an overview of Pb neurotoxicity at a resolution that has not previously been achievable. In the future, this could also be enhanced by using NIR-GECO [36].

4. Conclusions

In summary, this study demonstrates the use of versatile cell and animal models for the biosensing of Pb to provide an easily-to-use tool for advanced investigations into lead toxicology.

5. Materials and Methods

5.1. Cell culture

The human iPSC-derived cardiomyocytes (Human iPSC Cardiomyocytes - Cardiosight®-S) [24,25], were obtained from Nexel. A 96-well glass-bottom plate was first coated with 0.5% fibronectin/0.1% gelatin at 37°C for at least 1 h. The human iPSC cardiomyocytes were transferred into the plate wells and cultured for 3 days in Nexel's Cardiomyocyte Maintenance Medium, which was then replaced with Tyrode's buffer. For FRET imaging, the human cells were seeded onto 24-mm cover-glasses coated with poly-L-lysine and then transfected with Met-lead genes using Lipofectamine (Thermo Fisher Scientific) according to the manufacturer's instructions [20,26,27]. The cells were used for lead biosensing 2 days after transfection [23].

5.2. Fly strains and transgenic fly constructs

The *Drosophila melanogaster* stocks were raised on standard cornmeal medium and housed at 25°C with 70% relative humidity in a 12 h:12 h light:dark cycle incubator. To measure the contents of Pb within the cholinergic neurons of adult brains or the larval CNS, the strain *Cha-gal4* was used and was injected with *UAS-Met-lead 1.44 M1* [23,26].

5.3. Preparation or fly samples

For *in vivo* (rapid) time-lapse FRET biosensing of Pb in the adult fly brain, flies were placed into a custom-made plate and the brain of each fly was removed under the FRET

microscope [23]. For the larval CNS, each intact larva was cooled on ice and plated onto the FRET microscope for rapid image acquisition [26].

For *in vivo* (high-resolution, two-photon illumination) FRET biosensing of Pb within the larval CNS, whole larva bodies were immersed in 4% paraformaldehyde pre-cooled on ice and shaken gently for 1 h. The samples were transferred to 2% PBST (PBS with 2% Triton X-100) for 30 min and then shaken and placed in a vacuum chamber. The samples were then mounted onto coverslips and cleared with 15 μL RapiClear (SunJin Lab, Co, Taiwan), and were stored in an electronic dry cabinet until imaging.

5.4. FRET-based Pb imaging

For in-cell or *in vivo* FRET ratio imaging of Pb within iPSC-derived cardiomyocytes or in the *Drosophila* brain, an inverted microscope (Axiovert 200M, Zeiss, Germany) or a stereomicroscope (MVX-10, Olympus, Japan) equipped with a 440-nm light source and a W-View module (Gemini, Hamamatsu, Japan; with filters 542/27 nm for YFP and 483/32 nm for CFP) and a CMOS camera (ORCA-Flash4.0, Hamamatsu, Japan) controlled by HCImage software was used. The fluorescent signals of cp173Venus and ECFP(ΔC11) from samples that expressed Met-lead were rapidly acquired from the in-cell or *in vivo* FRET ratiometric imaging systems.

For the high-resolution FRET ratiometric imaging of larval CNS, a two-photon microscope was used. An 850-nm two-photon laser was applied as an excitation source within a multiphoton microscope (Zeiss LSM 7 MP, with 20×, NA 1.0 water objectives, Germany). The emission signals of YFP (530–630 nm) and CFP (460–500 nm) were acquired separately.

5.5. Data analysis

ImageJ was used to combine the ratio of fluorescent signals of cp173Venus (YFP channel) and ECFP(ΔC11) (CFP channel) using the Ratio Plus plugin and displayed with a rainbow-colored palette using the Lookup Table (LUT) to visualize FRET biosensing (colored from blue to red according to the lowest to the highest ratio value) within intact living cells, fly brains or the larval CNS.

References

1. Beattie, O.B.; Geiger, J. Frozen in Time: Unlocking the Secrets of the Franklin Expedition. 1987, Saskatoon: Western Producer Prairie Books. ISBN 978-0-88833-303-2.

2. Kowall, W.; Beattie, O.B.; Baadsgaard, H.; Krahn, P.M. Did solder kill Franklins men? *Nature* **1990**, 343, 319–320.

3. Kowall, W.A.; Krahnl, P.M. ; Beattie, O.B. Lead levels in human tissues from the Franklin Forensic Project. *Int. J. Environ. Anal. Chem.* **1988**, 35, 119–126.

4. Swanston, T.; Varney, T.L.; Kozachuk, M.; Choudhury, S.; Bewer, B.; Coulthard, I.; Keenleyside, A.; Nelson, A.; Martin, R.R.; Stenton, D. R.; et al; Franklin expedition lead exposure: New insights from high resolution confocal x-ray fluorescence imaging of skeletal microstructure. *PloS One* **2018**, 13, e0202983.

5. Martin, R.R.; Naftel, S.; Macfie, S.; Jones, K.; Nelson, A. Pb distribution in bones from the Franklin expedition: synchrotron X-ray fluorescence and laser ablation/mass spectroscopy. *Applied. Physics. A* **2013**, 111, 23–29.

6. Millar, K.; Bowman, A.; Battersby, W. A re-analysis of the supposed role of lead poisoning in Sir John Franklin's last expedition, 1845–1848 – CORRIGENDUM. *Polar. Record.* **2015**, 51, 341–342.

7. Smith K.E.; Weis, E.; Chauvel, C.; Moulin, S. Honey Maps the Pb Fallout from the 2019 Fire at Notre-Dame Cathedral, Paris: A Geochemical Perspective. *Envir. Sci. Tech. Lett.* **2020**, 7, 753-759.

8. Vallée, A.; Sorbets, E.; Lelong, H.; Langrand, J.; Blacher, J. The lead story of the fire at the Notre-Dame cathedral of Paris. *Environ. Pollut.* **2021**, 269, 116140.

9. Allonneau, A.; Mercier, S.; Maurin, O.; Robardet, F.; Menguy-Fleuriot, A.; Luu, S.C.; Louyot, C.; Jacques, N.; Jouffroy, R.; Prunet, B. Lead contamination among Paris Fire Brigade firefighters who fought the Notre Dame Cathedral fire in Paris. *Int. J. Hyg. Environ. Health* **2021**, 233, 113707.

10. Rocha, A.; Trujillo, K.A. Neurotoxicity of low-level lead exposure: History, mechanisms of action, and behavioral effects in humans and preclinical models. *Neurotoxicol.* **2019**, *73*, 58–80.

11. Lin, C.Y.; Huang, P.C.; Wu, C.; Sung, F.C.; Su, T.C. Association between urine lead levels and cardiovascular disease risk factors, carotid intima-media thickness and metabolic syndrome in adolescents and young adults. *Inter. J. Hygi. Eviron. Health* 2020, *223*, 248–255.

12. Mitra, P.; Sharma, S.; Purohit, P.; Sharma, P. Clinical and molecular aspects of lead toxicity: An update. *Crit. Rev. Clin. Lab. Sci.* **2017**, 54, 506-528.

13. Carter, K.P.; Young, A.M.; Palmer, A.E. Fluorescent sensors for measuring metal ions in living systems. *Chem. Rev.* **2014**, 114, 4564–4601.

14. Lai, C.; Zhang, Y.; Liu, X.; Liu, S.; Li, B.; Zhang, M.; Qin, L.; Yi, H.; Li, M.; Li, L.; Fu, Y.; He, J.; Chen, L. Electrochemical biosensor for amplified detection of Pb^{2+} based on perfect match of reduced graphene oxide-gold nanoparticles and single-stranded DNAzyme. *Anal. Bioanal. Chem.* **2019**, 411, 7499–509.

15. Miyawaki, A.; Llopis, J.; Heim, R.; McCaffery, J.M.; Adams, J.A.; Ikura, M.; Tsien, R.Y. Fluorescent indicators for Ca^{2+} based on green fluorescent proteins and calmodulin. *Nature*, **1997**, *388*, 882-887.

16. Hochreiter, B.; Garcia, A.P.; Schmid, J.A. Fluorescent proteins as genetically encoded FRET biosensors in life sciences. *Sensors* **2015**, 15, 26281–26314.

17. Zhang, X.; Hu, Y.; Yang, X.; Tang, Y.; Han, S.; Kang, A.; Deng, H.; Chi, Y.; Zhu, D.; Lu, Y. FÖrster resonance energy transfer (FRET)-based biosensors for biological applications. . *Biosen. Bioelec.* **2019**, 138, 111314.

18. Vinkenborg, J.L.; Nicolson, T.J.; Bellomo, E.A.; Koay, M.S.; Rutter, G.A.; Merkx, M. Genetically encoded FRET sensors to monitor intracellular Zn^{2+} homeostasis. *Nat. Method.* **2009**, 6, 737–740.

19. Wegner, S.V.; Arslan, H.; Sunbul, M.; Yin, J.; He, C. Dynamic copper(I) imaging in mammalian cells with a genetically encoded fluorescent copper(I) sensor. *J. Am. Chem. Soc.* **2010**, 132, 2567–2569.

20. Chiu, T.Y.; Yang, D.M. Intracellular Pb^{2+} content monitoring using a protein-based Pb^{2+} indicator. *Toxicol. Sci.* **2012**, *126*, 436-445.

21. Chiu, T.Y.; Chen, P.H.; Chang, C.L.; Yang, D.M. Live-cell dynamic sensing of Cd(2+) with a FRET-based indicator. *PloS One* **2013**, 8, e65853.

22. Chen, Y.-J.; Liu, C.-Y.; Tsai, D.-Y.; Yeh, Y.-C. A portable fluorescence resonance energy transfer biosensor for rapid detection of silver ions. *Sens. Actuators B* **2018**, *259*, 784–788.

23. Yang, D.M.; Fu, T.F.; Lin, C.S.; Chiu, T.Y.; Huang, C.C.; Huang, H.Y.; Chung, M.W.; Lin, Y.S.; Manurung, R.V.; Nguyen, P.; Chang, Y.F. High-performance FRET biosensors for single-cell and in vivo lead detection. *Biosen. Bioelec.* **2020**, 168, 112571.

24. Wang, Y.; Li, Z.C.; Zhang, P.; Poon, E.; Kong, C.W.; Boheler, K.R.; Huang, Y.; Li, R.A.; Yao, X. Nitric oxide-cGMP-PKG pathway acts on Orai1 to inhibit the hypertrophy of human embryonic stem cell-derived cardiomyocytes. *Stem Cell* **2015**, 33, 2973–2984.

25. Uzun, A.U.; Mannhardt, I.; Breckwoldt, K.; Horváth, A.; Johannsen, S.S.; Hansen, A.; Eschenhagen, T.; Christ, T. Ca^{2+}-currents in human induced pluripotent stem cell-derived cardiomyocytes effects of two different culture conditions. *Front. Pharmacol.* **2016**, 7, 300.

26. Yang, D.M.; Manurung, R.V.; Lin, Y.S.; Chiu, T.Y.; Lai, W.Q.; Chang, Y.F.; Fu, T.F. Monitoring the heavy metal lead inside

living Drosophila with a FRET-based biosensor. *Sensors* **2020**, 20, 1712.

27. Ferreira de Mattos, G.; Costa, C.; Savio, F.; Alonso, M.; Nicolson, G.L. Lead poisoning: acute exposure of the heart to lead ions promotes changes in cardiac function and Cav1.2 ion channels. *Biophys. Rev.* **2017**, 9, 807–825.

28. Lanphear, B.P.; Rauch, P.; Allen, R.W.; Hornung, R.W. Low-level lead exposure and mortality in US adults: a population-based cohort study. *Lancet Publich Health* **2018**, *3*, e177-e184.

29. Chang, Y.F.; Teng, H.C.; Cheng, S.Y.; Wang, C.T.; Chiou, S.H.; Kao, L.S.; Kao, F.J.; Chiou, A.; Yang, D.M. Orai1-STIM1 formed store-operated Ca^{2+} channels (SOCs) as the molecular components needed for Pb^{2+} entry in living cells. *Toxicol. Appl. Pharmacol.* **2008**, 227, 430-439.

30. Chiu, T.Y.; Teng, H.C.; Huang, P.C.; Kao, F.J.; Yang, D.M. Dominant role of Orai1 with STIM1 on the cytosolic entry and cytotoxicity of lead ions. *Toxicol. Sci.* **2009**, 110, 353-362.

31. Ferreira de Mattos, G.; Costa, C. Savio, F.; Alonso, M.; Nicolson, G.L. Lead poisoning: acute exposure of the heart to lead ions promotes changes in cardiac function and Cav1.2 ion channels. *Biophys. Rev.* **2017**, 9, 807–825.

32. Lin, C.Y.; Lee, H.L.; Hwang, Y.T.; Huang, P.C.; Wang, C.; Sung, F.C.; Wu, C.; Su, T.C. Urinary heavy metals, DNA methylation, and subclinical atherosclerosis. *Ecotoxicol. Envir. Safe.* **2020**, 204, 111039.

33. Besunder, J.B.; Super, D.M.; Anderson, R.L. Comparison of dimercaptosuccinic acid and calcium disodium ethylenediaminetetraacetic acid versus dimercaptopropanol and ethylenediaminetetraacetic acid in children with lead poisoning. *J Pediatrics* **1997**, 130, 966–971.

34. Bjørklund, G.; Mutter, J.; Aaseth, J. Metal chelators and neurotoxicity: lead, mercury, and arsenic. *Arch. Toxicol.* **2017**, 91, 3787–3797.

35. Qian, Y.; Piatkevich, K.D.; Mc Larney, B.; Abdelfattah, A.S.; Mehta, S.; Murdock, M.H.; Gottschalk, S.; Molina, R.S.; Zhang, W.; Chen, Y.; et al; A genetically encoded near-infrared fluorescent calcium ion indicator. *Nature Meth.* **2019**, 16, 171–174.

36. Qian, Y.; Cosio, D.; Piatkevich, K.D.; Aufmkolk, S.; Su, W.C.; Celiker, O.T.; Schohl, A.; Murdock, M. H.; Aggarwal, A.; Chang, Y.F.; et al; Improved genetically encoded near-infrared fluorescent calcium ion indicators for in vivo imaging. *PLoS Biol.* **2020**, 18, e3000965.